Maternal disruption of *Ube3a* leads to increased expression of *Ube3a-ATS* in *trans*

Miguel Landers, Margaret A. Calciano, Dan Colosi, Heather Glatt-Deeley, Joseph Wagstaff[1] and Marc Lalande*

Department of Genetics and Developmental Biology, University of Connecticut Health Center, Farmington, CT 06030-3301, USA and [1]Clinical Genetics Program, Carolinas Medical Center, Charlotte NC 28232-2861, USA

ABSTRACT

Angelman syndrome (AS) is a neurogenetic disorder characterized by severe mental retardation, 'puppet-like' ataxic gait with jerky arm movements, seizures, EEG abnormalities, hyperactivity and bouts of inappropriate laughter. Individuals with AS fail to inherit a normal active maternal copy of the gene encoding ubiquitin protein ligase E3A (UBE3A). UBE3A is transcribed predominantly from the maternal allele in brain, but is expressed from both alleles in most other tissues. It has been proposed that brain-specific silencing of the paternal UBE3A allele is mediated by a large (>500 kb) paternal non-coding antisense transcript (UBE3A-ATS). There are several other examples of imprinting regulation involving antisense transcripts that share two main properties: (i) the sense transcript is repressed by antisense and (ii) the interaction between sense and antisense occurs in *cis*. We show here that, in a mouse model of AS, maternal transmission of *Ube3a* mutation leads to increased expression of the paternal *Ube3a-ATS*, suggesting that the antisense is modulated by sense rather than the reciprocal mode of regulation. Our observation that *Ube3a* regulates expression of *Ube3a-ATS* in *trans* is in contrast to the other cases of sense–antisense epigenetic *cis*-interactions and argues against a major role for *Ube3a-ATS* in the imprinting of *Ube3a*.

INTRODUCTION

Epigenetic silencing via an antisense-mediated mechanism has been observed at the X-inactive specific transcript (*Xist*) and *Tsix* antisense locus (1) as well as for imprinted genes such as insulin-like growth factor-type-2 receptor (*Igf2r*) (2) and the potassium voltage-gated channel, KQT-like subfamily, member 1 (*Kcnq1*) (3,4). Silencing of the paternal alleles of *Igf2r* and *Kcnq1* is mediated by the paternal-specific non-coding antisense transcripts *Air* and *Kcn1qot1*, respectively. It has been shown that these antisense transcripts are regulated by differentially methylated regions (DMRs) since paternal deletion of the DMRs ablates expression of *Air* and *Kcn1qot1* (2–4). Truncation of the *Air* transcript not only results in loss of silencing of the paternal *Igf2r* allele, but also of two other paternal transcripts that are upstream of *Air* (5). There is evidence to suggest, however, that *Air* does not have a direct role in silencing *Igf2r* (6,7), based on the observation that *Igf2r* is not imprinted in the brain despite the paternal-specific expression of *Air* in this tissue (6). Moreover, it has been suggested that the mechanism of *Igf2r* imprinting involves parental allele-specific histone modifications at the *Igf2r* promoter rather than the action of *Air* and/or differential DNA methylation at the *Igf2r* locus (7). As a result, the concept that non-coding antisense transcripts have a direct role in regulating the expression of neighboring imprinted genes in *cis* remains controversial.

Like *Air* and *Kcn1qot1*, *Ube3a-ATS* is a paternal transcript that appears to be regulated by a DMR, the Prader–Willi syndrome imprinting center (PWS-IC) (8). It has been proposed that *Ube3a-ATS* is part of a long transcript (⩾500 kb) that initiates in the PWS-IC, a region that encompasses the *Snurf/Snrpn* promoter, and extends downstream (9–11). *Ube3a-ATS* is expressed in cultured neurons but not in glial cells (12), and its structure and organization is conserved in human, mouse and rat. Inheritance of a paternal deletion of the PWS-IC (ΔPWS-IC) abolishes transcription of all paternal transcripts in the region including small nuclear ribonucleo-protein N (*Snurf/Snrpn*) and *Ube3a-ATS* (8). A putative role for *Ube3a-ATS* in the *cis*-regulation of *Ube3a* imprinting is supported by the observation of increased expression of the paternal *Ube3a* allele in the ΔPWS-IC mice (8). One mechanism by which the PWS-IC regulates imprinting of

*To whom correspondence should be addressed. Tel: +1 860 679 8349; Fax: +1 860 679 8345; Email: lalande@uchc.edu

Ube3a-ATS could involve an interaction of the transcriptional repressor, methyl-CpG-binding protein 2 (MeCP2), with the maternal (methylated) PWS-IC locus. In this regard, *Ube3a* expression is observed to decrease in mutant mice that are deficient in MeCP2, with an associated change in *Ube3a-ATS* expression observed in one study (13) but not in the other (14). The question of whether *Ube3a-ATS* plays a role in *Ube3a* imprinting, therefore, remains unresolved. As an alternative approach to investigating the interaction between *Ube3a* and *Ube3a-ATS*, we analyzed the expression of *Ube3a-ATS* in mice bearing a targeted disruption of *Ube3a*.

Two mouse models of AS have been generated by targeted disruption of *Ube3a* (15,16). Upon inheritance of mutation through the maternal but not the paternal germline, both mutant mouse models display several features of AS. These include impaired motor function and long-term potentiation, deficits in context-dependent and spatial learning, inducible seizures, an abnormal hippocampal EEG and disruption of hippocampal calcium/calmodulin-dependent protein kinase II (CamKII) activity (15–17). In both mouse models, the inactive allele contained a reporter gene thus allowing the confirmation of a previous report (18) that maternal-specific expression occurs predominantly in hippocampal neurons and cerebellar Purkinje cells. Here, we examine the expression of *Ube3a* and *Ube3a-ATS* in brain from normal and mutant mice with the targeted disruption (16) of exons 12 and 13 (Figure 1). While disruption of the paternal *Ube3a* allele appeared to have no effect on paternal *Ube3a-ATS* expression, we were surprised to observe that disruption of the maternal *Ube3a* allele up-regulated the expression of the paternal antisense in *trans*.

MATERIALS AND METHODS

RNA preparation, cDNA synthesis and RT–PCR

Total RNA was isolated, using RNAzol (Tel-Test, Inc. Friendswood, TX), from mouse brain of B6, CAST and F1 offspring carrying either a maternally or a paternally transmitted mutant *Ube3a* allele (16) and from wild-type littermates. Reverse transcription reactions (+RT) were performed with 2 μg of RNA and Superscript reverse transcriptase (Invitrogen) using random hexamer primers or the *Ube3a-ATS* strand-specific primer E (5′-AGTTCTGGGAA-ATTGTTCATTCG-3′). A 2 μg aliquot of total RNA was incubated in a similar manner, but without reverse transcriptase (−RT) as a control. One twenty-fifth of the +RT or −RT reaction was used in PCR using *Taq* polymerase (Invitrogen) under conditions suggested by the manufacturer. Specific annealing temperatures and extension times are available upon request. Oligonucleotides for PCR (Figure 1) were as follows: C (5′-TTGTCAATCTCTATTCAGACTAC-3′); D (5′-CAACAGATTCCCTCGTATAGC-3′); F (5′-TTTAC-AGATGAACAGAAAAGACTC-3′); and G (5′-GTTTAC-AGCATGCCAAATCC-3′). The oligonucleotide primers and PCR conditions for *Gapdh* have been described previously (19).

Northern blot analysis

Twelve micrograms of total RNA was size-fractionated on a 1.2% agarose/formaldehyde gel and transferred to a Biotrans nylon membrane (ICN, Irvine, CA). Hybridization was performed in Expresshybe solution according to the manufacturer's (Clontech, Palo Alto, CA) specifications using the following probes: a 320 bp *Ube3a* cDNA probe from exons 5 and 6; an RT–PCR product from the distal *Ube3a* 3′-UTR [1.3 kb, using the M-1F/L-1R primer pair (11)] and a neomycin-specific probe. The *Ube3a-ATS*-specific probe was generated by PCR using the *Ube3a* intron 12-specific primers 5′-ACTTTGTACCCACTGTAAACC-3′ and 5′-CTTGATA-ACGTCTGTACTTCTG-3′. After washing, membranes were exposed to Kodak Biomax film and autoradiographed.

Allele-specific expression analysis

For conventional RT–PCR analysis (Figure 4), the parental alleles of *Ube3a-ATS* and *Atp10a* were distinguished using
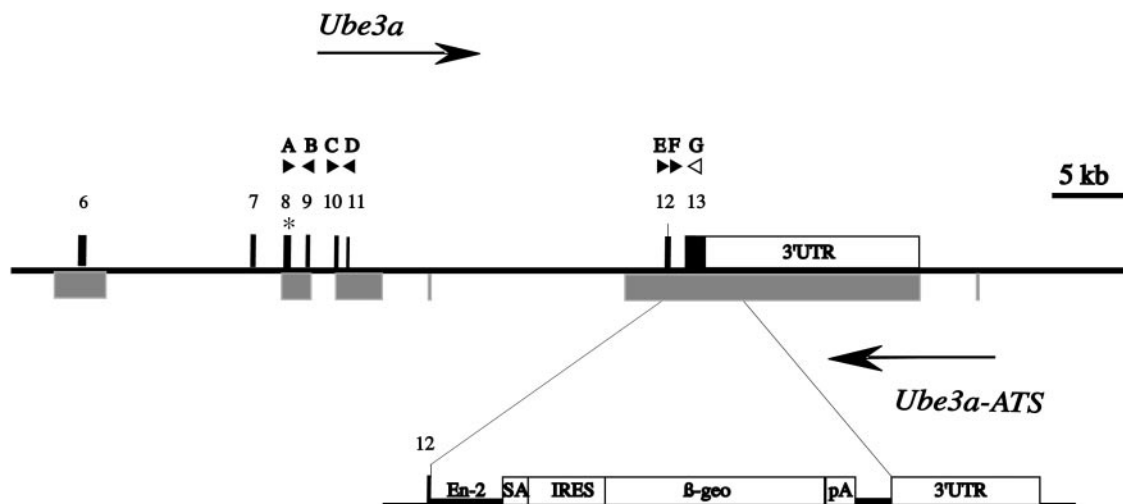
Figure 1. Partial map of *Ube3a* and *Ube3a-ATS* including the *Ube3a* targeting construct (16). Shaded regions under *Ube3a* exons indicate fragments of *Ube3a-ATS* that have been assayed for expression. Analysis of ESTs suggests that *Ube3a-ATS* spans most of the *Ube3a* gene including intronic regions. Horizontal arrow heads indicate positions of primers (A–G) used for RT–PCR expression studies; oligonucleotide primer G is deleted upon replacement by the targeting construct as denoted by the open arrow head. The asterisk (*) indicates the nucleotide polymorphism used for the allele-specific expression studies.

previously described polymorphisms (8,20). Allele-specific analysis of the *Ube3a* polymorphism (8) was performed using PCR oligonucleotide primers A (5′-AACTGAGGGTCAGTT-TACTCT-3′) and B (5′-AGATCATACATCATTGGGTTA-3′) (Figure 1).

Real-time PCR amplification (Figure 4B) of *Ube3a-ATS* in B6 and B6 × CAST maternal *Ube3a* mutation litters was carried out with the iQ™ SYBR® green Super mix using the iCycler iQ real-time detection system (Bio-Rad, Hercules, CA) with the following conditions: 95°C, 1 m; (94°C, 30 s; 60°C, 30 s; 72°C, 20 s) × 45; 72°C, 2 min. The specificity of the reactions was checked by melting curve profiles to monitor the presence of only one duplex DNA species and by agarose gel electrophoresis analysis of certain products to confirm the amplification of a single band of the expected size. The oligonucleotides for PCR were ATS-F (5′-TTGTATACAG-GAAGCTAATGGGG-3′) and ATS-R (5′-CAAAAGTTTAC-AAATAAATAATGTTCC-3′). Amplifications for RT+ and RT− samples were performed at least two times in triplicate with independent cDNA preparations and raw Ct values were obtained using iCycler iQ Optical System Software version 3.0. After normalizing *Ube3a-ATS* values to *Gapdh*, the comparative Ct method was used to calculate differences in expression levels between samples (21).

For the allelic discrimination analysis of the *Ube3a* locus in B6 × CAST and CAST × B6 cerebellum P55 RNA samples, a slightly modified TaqMan® assay (PE Applied Biosystems, Foster City, CA) was used. *Ube3a* maternal and paternal alleles were detected with the same nucleotide polymorphism as described above for allele-specific RFLP expression studies. Sequences of the PCR primers were as follows: Ube3aE×8-F (5′-GCATAGTCCTGGGTCTGGCTATT-3′) and Ube3aE×9-R (5′-AGATCTGTCTGTGATATCTGGAAAGTGA-3′). These primers were used together with modified oligonucleotide probes specific for B6 (5′-VIC-ACAATAA̱TTGTATACTGG-ATGTCC-MGB-3′) and CAST (5′-FAM-A̱CAATAA̱GTGT-ATACTGGATGTCC-MGB-3′). Amplifications were carried out with TaqMan® Universal PCR Master Mix (Roche, Branchburg, NJ) on an iCycler iQ real-time detection system (Bio-Rad) with the following conditions: 95°C, 3 m; (95°C, 15 s; 60°C, 1 m) × 60. Amplicons were analyzed at least two times in triplicate with independent cDNA preparations using iCycler iQ Optical System Software version 3.0 (Bio-Rad). The allelic discrimination function was used to plot and automatically call genotypes based on the fluorescence intensities of FAM and VIC at 49 cycles. Allelic discrimination plot values were further corrected with FAM and VIC fluorescence data obtained from B6 and CAST P55 cerebellum RNA included as controls in each plate assay to correct for cross-reactivity of the B6-specific VIC probe. The approach is validated by the consistency of the *Ube3a* parental expression ratios between wild-type reciprocal crosses (B × C +/+ and C × B +/+; Figure 5).

RESULTS

Northern blot analysis using a probe from the *Ube3a* coding region reveals a prominent doublet of ⩾10 kb and fainter 4.5–5.5 kb bands in normal m+/p+ brain (Figure 2A), a finding similar to that previously reported for *Ube3a* expression in normal tissues (22). In the *Ube3a* mutant mouse model studied here, the disrupted *Ube3a* transcript is detectable by northern blot hybridization (indicated by the * and ** in Figure 2A), consistent with expression of the lacZ reporter from the targeted allele in brain tissue sections (16). The smaller (*) re-arranged mRNA (Figure 2A) most probably represents the *Ube3a*-LacZ-neo transcript since this fragment is not detected by a probe from the distal *Ube3a* 3′-UTR (Figure 2B), but is detected by a neomycin-specific probe (Figure 2C). The larger (**) re-arranged mRNA, however, appears to use an endogenous termination signal in the *Ube3a* 3′-UTR since it is detected by both the probe from the *Ube3a* 3′ non-coding region (Figure 2B) and by the *neo* probe (Figure 2C).

The re-arranged transcripts (* and **, Figure 2A) are highly prominent in the brain sample from mice with the maternal disruption (m−/p+) of the *Ube3a* allele, but very faint in the m+/p− sample (Figure 2A). The greater expression of the re-arranged transcripts in m−/p+ compared to m+/p− corresponds to the predominant transcription of the targeted maternal (m−) allele in brain. Similarly, the normal ⩾10 kb doublet predominates in m+/p− brain as a result of maternal-specific expression of the normal *Ube3a* (m+) allele in this sample. Densitometric analysis of the maternal- and paternal-specific hybridization bands detected using the *Ube3a* and *neo* probes (Figure 2A and C) reveals a >10-fold maternal:paternal allele expression ratio for *Ube3a*. A similar ratio is also observed in a replicate northern blot experiment (data not shown). The strong bias (⩾10:1) towards maternal expression in brain is difficult to reconcile with previous observations of *Ube3a* imprinting in a relatively limited number of neuronal tissues (15,16,18).

The *Ube3a-ATS* is a large and complex transcript that initiates upstream of *Snrpn* and extends to overlap most of the *Ube3a* transcript (9,11). In order to distinguish between *Ube3a* and *Ube3a-ATS* by northern blot hybridization, we generated an *Ube3a* intron 12-specific probe by PCR. Hybridization with the intron 12-specific probe reveals a smear in m+/p+ and m−/p+ but not in m+/p− brain samples (Figure 2D) suggesting that this probe is specific for *Ube3a-ATS*. The hybridization smear is typical of natural antisense transcripts (23) and has previously been observed using the *Ube3a-ATS* probe, *Ipw* (24). Because intron 12 is deleted in the targeted allele and since *Ube3a-ATS* displays paternal-specific expression, hybridization of the intron 12-specific probe is only detected in those samples with a normal paternal (p+) allele (Figure 2D). Examination of the intensity of the *Ube3a-ATS* hybridization signals in Figure 2D suggested an increase in the m−/p+ relative to the m+/p+ sample. We measured the total hybridization signal in these samples by densitometry and obtained a value of 2.9 for the ratio of the m−/p+ to the m+/p+ signals (normalized to the gel densitometric measurement of 28S bands). A similar analyis of a replicate experiment (data not shown) gave a ratio of 1.8.

These findings suggested that disruption of the maternal *Ube3a* allele could affect the paternal-specific expression of *Ube3a-ATS*. In order to investigate the possibility of this *trans* interaction between sense and antisense, we performed semi-quantitative RT–PCR using primers for different regions of overlap between *Ube3a* and *Ube3a-ATS*. Total brain RNA from mutant and normal mice analyzed by RT–PCR using primers F and G (Figure 1) in exons 12 and 13, respectively,
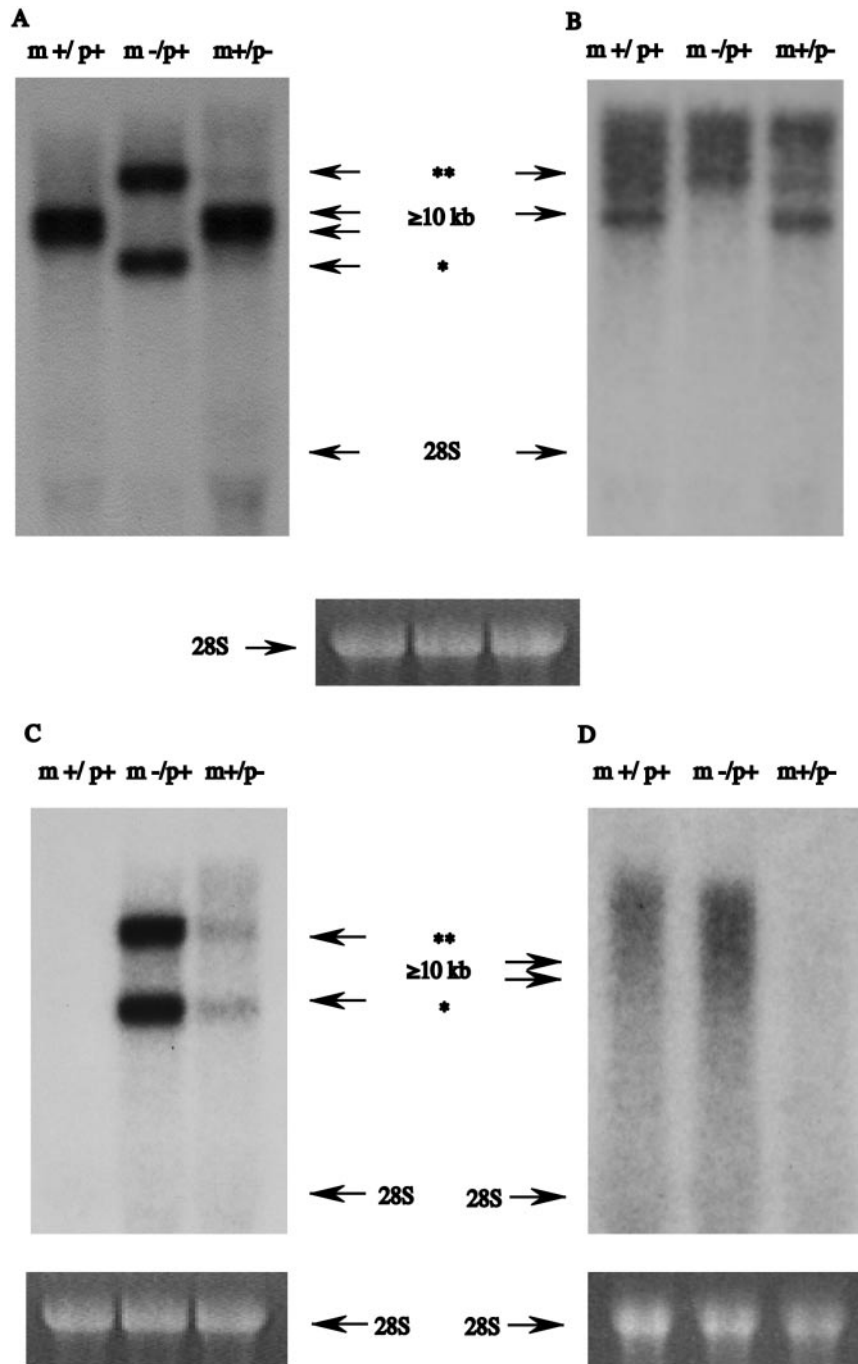
Figure 2. Northern blot analysis of *Ube3a* in m+/p+, m−/p+ and m+/p− brain. (**A**) Hybridization with an *Ube3a* cDNA probe. The doublet of hybridization bands at ≥10 kb corresponds to normal (non-targeted) *Ube3a* transcripts while the re-arranged transcripts are indicated by an asterisk. (**B**) The blot from A is re-hybridized with a probe from the distal *Ube3a* 3′-UTR that hybridizes to both *Ube3a* and *Ube3a-ATS*. The background smear results, at least in part, from multiple *Ube3a-ATS* splice forms. The smaller (*) *Ube3a* re-arranged transcript is not detected using this probe suggesting that the (*) transcript corresponds to the major *Ube3a*-LacZ-neo fusion transcript that uses the polyadenylation site of the targeting construct (Figure 1). The larger (**) fragment, however, is detected using the *Ube3a* 3′-UTR probe suggesting that this re-arranged *Ube3a* transcript terminates in the distal 3′-UTR. (**C**) Consistent with this suggestion, a neomycin-specific probe detects both (* and **) re-arranged transcripts. (**D**) Hybridization of a probe from *Ube3a* intron 12 reveals a smear in m+/p+ and m−/p+ but not in m+/p− brain samples. The smear results from hybridization of the intron 12 probe to the paternal *Ube3a-ATS* allele in the m+/p+ and m−/p+ samples. The absence of a hybridization smear in the m+/p− RNA is because intron 12 is deleted in the targeted paternal allele. The 28S ribosomal RNAs serve as a sample loading control.

is shown in Figure 3A. Two products are detected; one of 244 bp corresponding to the *Ube3a* exons 12 and 13, and one of 1200 bp that is the unspliced *Ube3a-ATS* containing intron 12 (Figure 3A). Only the normal (non-targeted) *Ube3a*

and *Ube3a-ATS* alleles are detected in this analysis since primer G is specific for the part of exon 13 that is deleted upon replacement by the targeting cassette. *Ube3a* levels are significantly reduced in the m−/p+ relative to the m+/p+
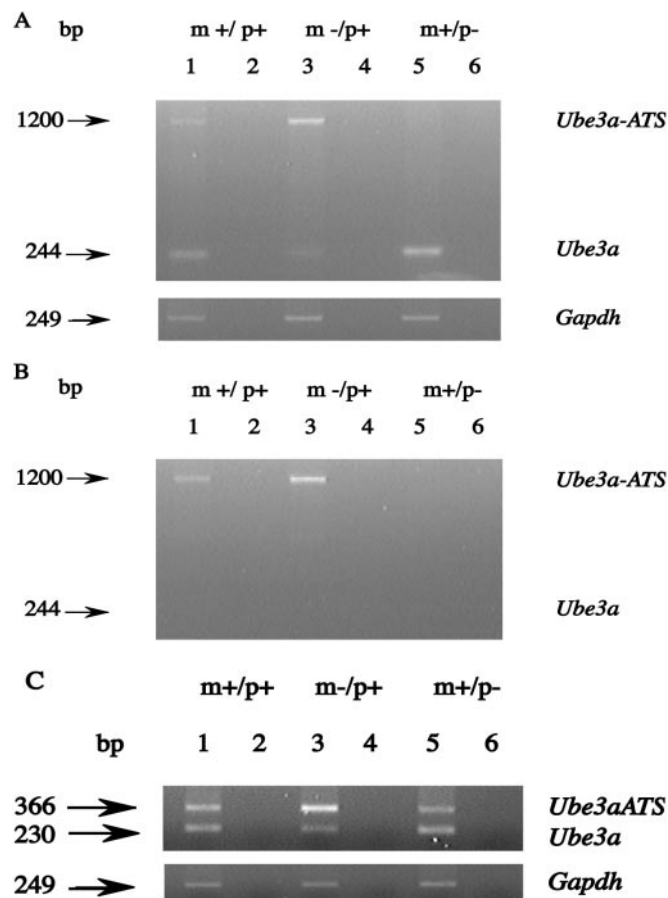
Figure 3. RT–PCR expression analysis of *Ube3a* and *Ube3a-ATS* in normal and mutant mouse brain. Lanes 1 (+RT) and 2 (−RT), m+/p+; lanes 3 (+RT) and 4 (−RT), m−/p+; lanes 5 (+RT) and 6 (−RT), m+/p−. (**A** and **B**) Analysis using the F–G primer pair that detects normal (non-targeted) *Ube3a* exons 12 and 13 (244 bp) and the unspliced *Ube3a-ATS* spanning intron 12 (1200 bp). The RT reaction was primed using random hexamers (A) or the strand-specific primer E (B). (**C**) Analysis using the C–D primer pair specific for exons 10 and 11 yields 230 and 366 bp products for *Ube3a* and *Ube3a-ATS*, respectively, upon RT primed with random hexamers. The identity of all *Ube3a-ATS* and *Ube3a* products were confirmed by nucleotide sequencing. Glyceraldehyde-3-phosphate dehydrogenase (*Gapdh*) expression was used as a control.

and m+/p− samples (compare lane 3 to lanes 1 and 5, Figure 3A), a finding consistent with the observation that the paternal *Ube3a* allele is repressed in brain (15,16,18).

To confirm that the 1200 bp corresponds to *Ube3a-ATS*, we performed an RT with the antisense strand-specific primer E, followed by PCR with the F and G oligonucleotides (Figure 3B). Only the 1200 bp product is detected in Figure 3B, confirming that this is the *Ube3a-ATS* product. The analysis of *Ube3a-ATS* expression (Figure 3A and B) confirms that the antisense is exclusively paternal in brain since RT–PCR products are detectable in the RNA samples from maternal *Ube3a*-deficient (m−/p+) mice and control littermates (m+/p+) but not from paternal-deficient (m+/p−) animals.

We also examined *Ube3a-ATS* expression across exons 10 and 11, a region of *Ube3a* that is not replaced by gene targeting, by RT–PCR using primers C and D (Figure 3C). In this RT–PCR analysis, the 230 bp band size corresponds to the *Ube3a* exon 10/11 splice product while the 366 bp band

size results from the unspliced *Ube3a-ATS* containing intron 10 (Figure 3C). *Ube3a-ATS* is observed in all three samples indicating that the targeted paternal deletion of exons 12 and 13 does not eliminate expression of the antisense in upstream regions of *Ube3a* overlap. Another important feature of the analysis in Figure 3C is the markedly increased levels of expression of *Ube3a-ATS* that are observed in the m−/p+ relative to the m+/p+ control littermate and the m+/p− sample. The increased *Ube3a-ATS* expression in m−/p+ brain is also evident in intron 12 (compare intensity of 1200 bp products in lanes 1 and 3, Figure 3A and B). Replicate RT–PCR experiments indicated that the level of *Ube3a-ATS* was increased at least 2-fold in the m−/p+ relative to m+/p+ brain, a ratio that is similar to that obtained by northern blot analysis (Figure 2D). The results of *Ube3a–ATS* expression analysis (Figures 2 and 3) strongly suggest that disruption of the maternal *Ube3a* allele affects the levels of *Ube3a-ATS* expression in *trans*. To further confirm the putative *trans* sense/antisense interaction, we performed *Ube3a-ATS* analysis on a different mouse strain background by crossing C57Bl/6J (B6) mice carrying the targeted *Ube3a* allele to *M.m.castaneus* (CAST/Ei) animals.

We exploited a Tsp509I restriction fragment polymorphism in *Ube3a* exon 8 (*, Figure 1) (8) to analyze the sense and antisense expression in cerebellum of C57Bl/6J (B6), CAST/Ei (CAST) and F1 offspring of CAST × B6 and B6 × CAST crosses (Figure 4A). There are two Tsp509I sites in the B6 *Ube3a* exon 8 versus a single one in CAST (8). To amplify *Ube3a-ATS* by RT–PCR, a forward primer upstream of the Tsp509I restriction sites in exon 8 is used in combination with a reverse primer from intron 8 (8). The expression of *Ube3a-ATS* using template RNA from cerebellum of 7.5-week-old mice is summarized in the top panel of Figure 4A. The 840 bp *Ube3a-ATS* product (lanes 1, 3, 5, 7, 9 and 11) yields sizes of 553 and 640 bp (smaller products not shown), respectively, for the B6 (lane 2) and CAST (lane 4) alleles upon cleavage with Tsp509I. Paternal-specific expression of *Ube3a-ATS* is evident in both the +/+ hybrid crosses (lanes 6 and 12) and in the mice that derive the *Ube3a* mutation from either B6 parent (lanes 8 and 10). These findings confirm that inheritance of the *Ube3a* mutation does not affect the paternal-specific expression pattern of *Ube3a-ATS*. Again, increased expression of *Ube3a-ATS* is evident in B6 × CAST m−/p+ relative to B6 × CAST m+/p+ cerebellum for the samples either cleaved with Tsp509I (compare lanes 8 and 6) or not treated with the restriction enzyme (compare lanes 7 and 5). These experiments also suggest that the CAST *Ube3a-ATS* allele is expressed at a higher level than that of the B6 (compare lane 3 to 1, top panel, Figure 4A).

The allele-specific expression of *Ube3a* in cerebellum is shown in the second panel of Figure 4A. A forward primer (A, Figure 1) upstream of the B6-specific Tsp509I restriction site and a reverse primer (B, Figure 1) in exon 9 (11) are used for allele-specific RT–PCR. The RT–PCR product using the *Ube3a* primer pair is 300 bp in size (lanes 1, 3, 5, 7, 9 and 11). Upon Tsp509I digestion of the resulting RT–PCR products, the CAST allele (300 bp) is not cleaved (lanes 3 and 4) whereas the B6 allele digests to yield a 200 bp fragment (lanes 1 and 2, smaller product not seen). The predominant expression of the maternal *Ube3a* allele is evident in all crosses upon analysis of Tsp509I restriction of RT–PCR
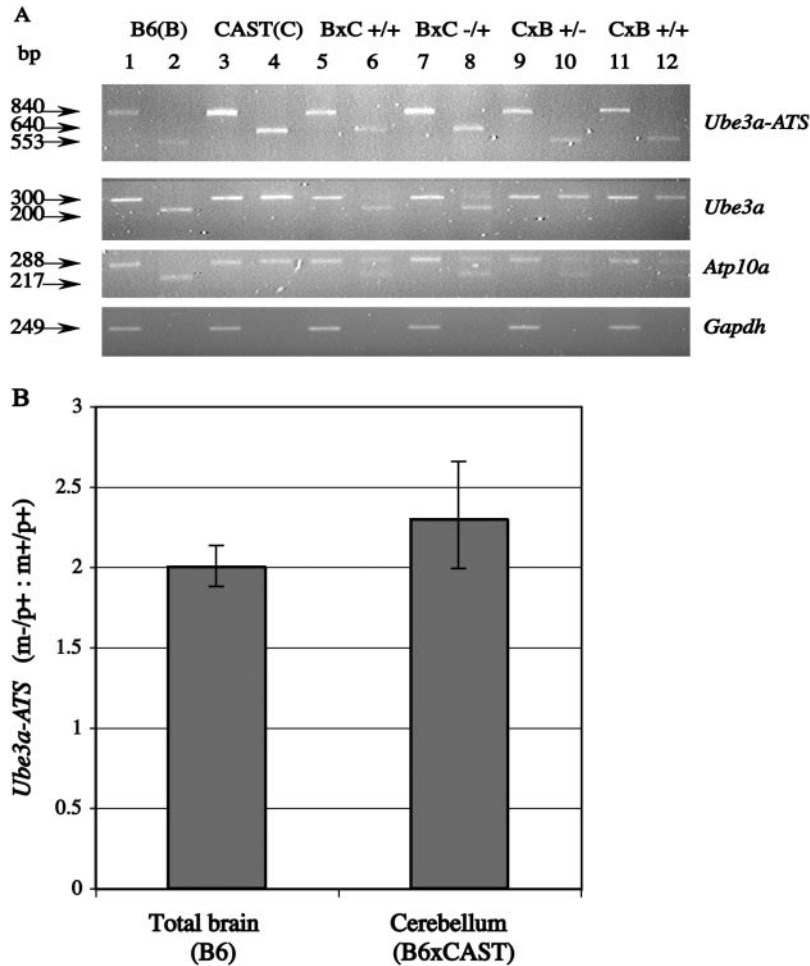
Figure 4. (**A**) Allele-specific RT–PCR expression analysis of *Ube3a-ATS, Ube3a* and *Atp10a*. RNA is extracted from the cerebellum of B6, CAST and the reciprocal F1 crosses: B6 × CAST (B × C) and CAST × B6 (C × B). The mutant *Ube3a* (−) allele is carried on the B6 background. The samples are subjected to RT–PCR analysis using primers that span a restriction enzyme polymorphism. RT–PCR fragments are divided into two aliquots that are either untreated (lanes 1, 3, 5, 7, 9 and 11) or cleaved with the diagnostic restriction enzyme (lanes 2, 4, 6, 8, 10 and 12). RT–PCR analysis of *Ube3a-ATS* is performed with primers in *Ube3a* exon 8 and intron 8, while primers in exon 8 and exon 9 (8) are used for *Ube3a* expression analysis (see text for details). Allele-specific analysis of *Atp10a* is based on the previously described MspI polymorphism (20). The B6 and CAST *Ube3a-ATS* alleles are detected as 553 and 640 bp fragments, respectively, upon Tsp509I digestion (8). Only the paternal *Ube3a-ATS* allele is detected in the mutant (lanes 8 and 10) and normal (lanes 6 and 12) samples. For *Ube3a* analysis, the B6 (200 bp) and CAST (300 bp) alleles are resolved after treatment with Tsp509I. *Ube3a* expression is predominantly maternal (lanes 6, 8, 10 and 12) in cerebellum. The B6 and CAST *Atp10a* alleles, corresponding to the 217 and 288 bp products, respectively, appear to show near equal levels of expression (lanes 6, 8, 10 and 12) suggesting bi-allelic expression of *Atp10a*. The *Gapdh* control is shown in the bottom panel. (**B**) Quantitative RT–PCR analysis of the *Ube3a-ATS* expression in normal and mutant mouse samples. Real-time RT–PCR amplification of *Ube3a-ATS* is performed using RNA from total B6 brain and from B6 × CAST cerebellum. The analysis is carried out with the iQ™ SYBR® green Super mix and iCycler iQ real-time detection system using the mutant (m−/p+) and normal (m+/p+) samples. The experiment is performed at least two times in triplicate with independent cDNA preparations and normalized to the *Gapdh* control. The histograms represent the ratio of *Ube3a-ATS* expression in the m−/p+ mutant relative to the m+/p+ control.

products (compare intensity of 200 and 300 bp products in lanes 6, 8, 10 and 12, second panel, Figure 4A). We also examined the allele-specific expression of the P-type ATPase *Atp10a* in these samples (third panel, Figure 4A). *Atp10a* maps ∼500 kb downstream of *Ube3a* on mouse chromosome 7C (25) and displays predominantly maternal expression in human (26). In mouse, *Atp10a* has been reported to be both bi-allelic (27) and maternal-specific (20), suggesting the possibility of strain-dependent imprinting of *Atp10a* (28). Allele-specific expression of *Atp10a* was performed as described previously (20) using a B6-specific MspI restriction site to distinguish the B6 and CAST alleles. RT–PCR analysis of *Atp10a* using these primers yields a 288 bp product (lanes 1, 3, 5, 7, 9 and 11) with the B6 allele identified by the 217 bp

size band upon MspI digestion (lane 2). The two parental alleles display roughly equal levels (compare the intensity of 288 and 217 bp bands in lanes 6, 8, 10 and 12, Figure 4A, third panel) suggesting bi-allelic expression rather than predominantly maternal expression in cerebellum.

We then used quantitative PCR (qPCR) to measure *Ube3a-ATS* expression levels in the mutant and normal mice (Figure 4B). We quantified the levels of *Ube3a-ATS* in total brain of 3.5-week-old m−/p+ and m+/p+ B6 mice using primers from exon 8 and intron 8 for RT–qPCR. This analysis reveals a 2-fold increase of *Ube3a-ATS* levels in the m−/p+ relative to m+/p+ (Figure 4B) and confirms the results obtained by northern blot analysis (Figure 2D) and conventional RT–PCR analysis (Figure 3). A ⩾2-fold increase in
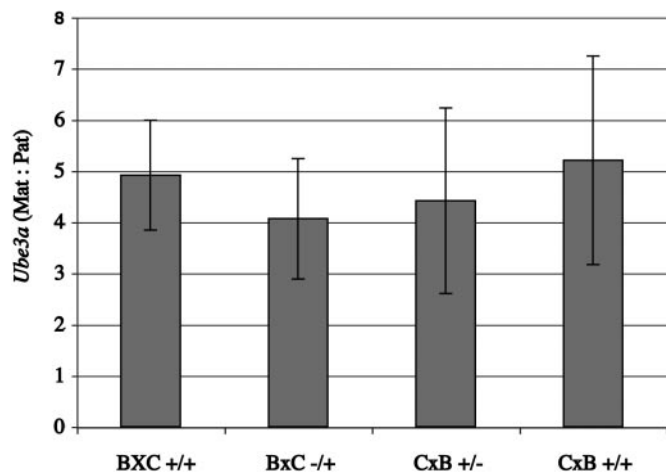
Figure 5. Quantitative PCR analysis of *Ube3a* expression in normal and mutant mouse samples. Allele-specific expression of *Ube3a* in cerebellum by qPCR analysis of the T/G polymorphism (also detectable with Tsp509I in Figure 4). The T-B6-specific and G-CAST-specific probes are labeled at their 5′ end with the VIC and FAM fluorophores, respectively. PCR amplifications are carried out with the VIC and FAM probe using the TaqMan Universal PCR Master Mix on an iCycler iQ real-time detection system. Each amplicon is analyzed at least two times in triplicate with independent cDNA preparations and the maternal: paternal *Ube3a* allele expression ratios are calculated for the B × C m+/p+, B × C m−/p+, C × B m−/p+ and C × B m+/p+ cerebellum samples.

the level of *Ube3a-ATS* is also observed in the cerebellum of 7.5-week-old m−/p+ B6 × CAST F1 offspring relative to B6 × CAST F1 m+/p+ littermates (Figure 4B), a result again indicating that maternal disruption of *Ube3a* elevates the expression of *Ube3a-ATS* in *trans*.

Based on the current hypothesis that *Ube3a-ATS* represses *Ube3a* in *cis*, we might expect that the 2- to 3-fold increase in *Ube3a-ATS* levels, that are observed in m−/p+ brain (Figures 2–4), will decrease the paternal *Ube3a* mRNA. To address this question, we measured the ratio of maternal: paternal expression of *Ube3a* by qPCR in m−/p+ and m+/p+ cerebellum (Figure 5). If increased *Ube3a-ATS* expression reduces paternal *Ube3a* mRNA levels in *cis*, the maternal:paternal allele *Ube3a* expression ratio should increase in the m−/p+ relative to the m+/p+ sample. The results of Figure 5 show that this is not the case since these ratios do not significantly vary in m−/p+ and m+/p+ cerebellum. For these experiments, we designed probes specific for the SNP corresponding to the Tsp509I polymorphism in *Ube3a* exon 8. The probes were used to measure, by Taqman qPCR, the expression levels of the B6 and CAST *Ube3a* alleles in 7.5-week-old mutant and normal B6 × CAST and CAST × B6 offspring (Figure 5). These experiments indicate that the ratio of expression of the maternal:paternal allele is similar (∼4:1) in all crosses suggesting that increased expression of paternal *Ube3a-ATS* has no effect in *cis* on the levels of *Ube3a* mRNA.

DISCUSSION

We report here that the maternal disruption of *Ube3a* causes an up-regulation of the paternal *Ube3a-ATS*. In contrast to other examples of epigenetic silencing involving the repression of sense by the antisense in *cis*, this observation indicates that

there is *trans* interaction between *Ube3a* and *Ube3a-ATS*. Another important finding is that the *trans* interaction involves modulation of the antisense by the sense rather than the reciprocal as has been reported in cases of epigenetic silencing of a sense transcript by a non-coding antisense RNA.

A role for *trans* effects in the regulation of imprinting was first suggested by the observation of a physical association between the homologous 15q11–q13 regions during interphase in human cells (29). Moreover, cells of PWS and AS individuals were deficient in homologous association, suggesting that this process might be involved in the establishment and/or maintenance of imprinting (29). Data supporting the physical association of oppositely imprinted 15q11–q13 chromosomal domains were reported in one study (30) but not in another (31), while homologous association of the oppositely imprinted regions of distal mouse chromosome 7 has also been observed (32). It was suggested that homologous association was not required for normal imprinting in a transgenic insertion mouse model of AS/PWS (33). On the other hand, the study of uniparental fetuses has suggested that both parental genomes are required to establish maternal-specific expression of *Igf2r* (34). There are also several reports of the transfer of the DNA methylation patterns between alleles in gene targeting experiments at both imprinted and non-imprinted loci (35–39). Strong evidence for the involvement of *trans*-interactions in the imprinting at the AS/PWS locus was reported upon gene targeting of *Snurf/Snrpn* (40). In the latter study, inactivation of the paternal *Snurf/Snrpn* allele resulted in partial or complete demethylation of the maternal allele, indicating that imprint switching can occur in *trans* upon disruption of the paternal copy of *Snurf/Snrpn* (40).

In terms of mechanisms involved in the *trans* interaction between *Ube3a* and *Ube3a-ATS*, one possibility is that the *Ube3a* gene product normally functions to repress *Ube3a-ATS* expression, perhaps via pathways that involve ubiquitination and chromatin silencing. Brain-specific expression of *Ube3a-ATS* is controlled by the PWS-IC and additional upstream exons distributed within an ∼500 kb region upstream of *Snrpn* (8,11). Targeted disruption of the maternal *Ube3a* allele and the resulting diminution of *Ube3a* protein could impede an *Ube3a*-mediated chromatin silencing process in the *Snrpn* upstream region and result in the up-regulation of *Ube3a-ATS* in *trans*. In this regard, recruitment of an E3 ligase has been shown to be involved in the regulation of gene silencing in *Saccharomyces cerevisiae* (41). There is currently no evidence, however, suggesting that *Ube3a* is involved in histone ubiquitination or in other aspects of chromatin silencing.

Another mechanism could involve a direct interaction between the *Ube3a* and *Ube3a-ATS* RNAs. In this regard, the formation of duplexes between complementary sense and antisense transcripts from different chromosomes has recently been demonstrated for the ribosomal S2 and S9 proteins and for Keratin 8 (42). Annealing of the complementary maternal sense to the paternal antisense RNA strands could regulate expression in several ways. One possibility is that a double strand formed between sense and antisense would decrease the stability of *Ube3a* and *Ube3a-ATS*. In this scenario, the replacement of *Ube3a* by the targeting construct would disrupt duplex formation between sense and antisense strands in *trans* and thereby stabilize the *Ube3a-ATS* RNA in m−/p+ brain. RNA editing or RNA interference (RNAi)

might be involved in the aforementioned dsRNA degradation, although both processes would be predicted to affect the levels of both sense and antisense. While the hypothesis needs to be tested in individual neurons, our qPCR data (Figure 5) appear to be inconsistent with the involvement of dsRNA degradation by RNAi or RNA editing since the increase in *Ube3a-ATS* observed in the m−/p+ brain does not appear to be associated with a coordinated increase in the levels of the maternal (targeted) *Ube3a* allele.

The modulation of *Ube3a-ATS* by *Ube3a* in *trans* contrasts with the other reported cases of epigenetic silencing that involve *cis*-repression of sense by the antisense. The *cis* and *trans* modes of sense/antisense coupling could be associated with differences in function. The *cis*-interaction between *Xist* and *Tsix* is characterized by a 10–100 times excess of antisense over sense (43,44), whereas we observe no such increase in steady-state *Ube3a-ATS* levels relative to *Ube3a*. It has also been shown that both *Xist* and *Tsix* are nuclear transcripts and their *cis*-interaction is constrained by their tight association with a single X chromosome (1). The putative *trans* interaction for *Ube3a* could result from the absence of any local association of sense and antisense with chromosome 7 or be due to localization outside the nucleus. In this regard, detailed *in situ* hybridization experiments in mouse brain have revealed a mainly cytoplasmic localization for one *Ube3a-ATS* splice form that overlaps *Ube3a* (E. Le Meur, F. Watrin, M. Landers, R. Sturny, M. Lalande and F. Muscatelli, submitted for publication). These findings suggest *Ube3a* sense and antisense can interact in the cytoplasm and raise the possibility that *Ube3a-ATS* functions in the post-transcriptional control rather than the epigenetic regulation of *Ube3a*.

Using a hybridization probe from *Ube3a* intron 12, we observe a high molecular weight smear in the m+/p+ and m−/p+ brain samples upon northern blot analysis (Figure 2D). This finding is entirely consistent with previous reports indicating that *Ube3a-ATS* is a large (>500 kb) alternatively processed paternal-specific transcript that overlaps *Ube3a* (9,11). In line with the current hypothesis, these observations suggest that the brain-specific *Ube3a-ATS* could function to silence the paternal *Ube3a* allele in *cis*. While our results do not directly address antisense function, it is clear that the increased expression of *Ube3a-ATS* in m−/p+ brain does not affect the steady-state level of the paternal *Ube3a* allele (Figure 5). Our findings are, therefore, inconsistent with a simple model whereby increased *Ube3a-ATS* expression results in a corresponding decrease in *Ube3a* RNA in *cis* and argue that elements other than *Ube3a-ATS* control the allele-specific expression of *Ube3a*. In support of this hypothesis, RNA-FISH analysis suggests a preferential maternal UBE3A expression in non-neuronal human tissues, such as fibroblasts and lymphoblasts, where UBE3A-ATS is not expressed (30).

Finally, our allele-specific expression analysis of *Ube3a* in brain reveals a very significant bias for maternal expression (Figures 2 and 4). While a rough estimate of 2:1 for the maternal:paternal allele-specific expression ratio was previously obtained by RT–PCR using total brain RNA (8), our northern blot analysis indicates that the *Ube3a* maternal:paternal expression ratio is ≥10:1 in total brain (Figure 2 and data not shown). Despite the differences in the values obtained by RT–PCR and northern blot analysis, the results seem

surprising given that imprinting of *Ube3a* has been reported to be restricted mainly to hippocampal neurons and the Purkinje cells of the cerebellum (15,18). In this regard, the disrupted *Ube3a* allele in our mutant mice contains a *lacZ* reporter gene thereby permitting an analysis of the allele-specific expression of *Ube3a* in different brain regions (16). Visualization of the β-galactosidase activity in mice upon maternal and paternal inheritance of the disrupted allele reveals that *Ube3a* is imprinted in hippocampus and cerebellum (16), a result consistent with previous studies. While these histochemical and *in situ* hybridization studies suggest a near-complete repression of the paternal *Ube3a* allele in hippocampus and cerebellum, our experiments strongly suggest that there is a marked bias for maternal expression throughout most regions of brain.

REFERENCES

1. Lee,J.T., Davidow,L.S. and Warshawsky,D. (1999) Tsix, a gene antisense to Xist at the X-inactivation centre. *Nature Genet.*, **21**, 400–404.
2. Wutz,A., Smrzka,O.W., Schweifer,N., Schellander,K., Wagner,E.F. and Barlow,D.P. (1997) Imprinted expression of the *Igf2r* gene depends on an intronic CpG island. *Nature*, **389**, 745–749.
3. Fitzpatrick,G.V., Soloway,P.D. and Higgins,M.J. (2002) Regional loss of imprinting and growth deficiency in mice with a targeted deletion of KvDMR1. *Nature Genet.*, **32**, 426–431.
4. Horike,S., Mitsuya,K., Meguro,M., Kotobuki,N., Kashiwagi,A., Notsu,T., Schulz,T.C., Shirayoshi,Y. and Oshimura,M. (2000) Targeted disruption of the human LIT1 locus defines a putative imprinting control element playing an essential role in Beckwith–Wiedemann syndrome. *Hum. Mol. Genet.*, **9**, 2075–2083.
5. Sleutels,F., Zwart,R. and Barlow,D.P. (2002) The non-coding Air RNA is required for silencing autosomal imprinted genes. *Nature*, **415**, 810–813.
6. Hu,J.F., Balaguru,K.A., Ivaturi,R.D., Oruganti,H., Li,T., Nguyen,B.T., Vu,T.H. and Hoffman,A.R. (1999) Lack of reciprocal genomic imprinting of sense and antisense RNA of mouse insulin-like growth factor II receptor in the central nervous system. *Biochem. Biophys. Res. Commun.*, **257**, 604–608.
7. Vu,T.H., Li,T. and Hoffman,A.R. (2004) Promoter-restricted histone code, not the differentially methylated DNA regions or antisense transcripts, marks the imprinting status of IGF2R in human and mouse. *Hum. Mol. Genet.*, **13**, 2233–2245.
8. Chamberlain,S.J. and Brannan,C.I. (2001) The Prader–Willi syndrome imprinting center activates the paternally expressed murine Ube3a antisense transcript but represses paternal Ube3a. *Genomics*, **73**, 316–322.
9. Runte,M., Huttenhofer,A., Gross,S., Kiefmann,M., Horsthemke,B. and Buiting,K. (2001) The IC-SNURF-SNRPN transcript serves as a host for multiple small nucleolar RNA species and as an antisense RNA for UBE3A. *Hum. Mol. Genet.*, **10**, 2687–2700.
10. Runte,M., Kroisel,P.M., Gillessen-Kaesbach,G., Varon,R., Horn,D., Cohen,M.Y., Wagstaff,J., Horsthemke,B. and Buiting,K. (2004) SNURF-SNRPN and UBE3A transcript levels in patients with Angelman syndrome. *Hum. Genet.*, **114**, 553–561.
11. Landers,M., Bancescu,D.L., Le Meur,E., Rougeulle,C., Glatt-Deeley,H., Brannan,C., Muscatelli,F. and Lalande,M. (2004) Regulation of the large (approximately 1000 kb) imprinted murine Ube3a antisense transcript by alternative exons upstream of Snurf/Snrpn. *Nucleic Acids Res.*, **32**, 3480–3492.

12. Yamasaki,K., Joh,K., Ohta,T., Masuzaki,H., Ishimaru,T., Mukai,T., Niikawa,N., Ogawa,M., Wagstaff,J. and Kishino,T. (2003) Neurons but not glial cells show reciprocal imprinting of sense and antisense transcripts of Ube3a. *Hum. Mol. Genet.*, **12**, 837–847.

13. Makedonski,K., Abuhatzira,L., Kaufman,Y., Razin,A. and Shemer,R. (2005) MeCP2 deficiency in Rett syndrome causes epigenetic aberrations at the PWS/AS imprinting center that affects UBE3A expression. *Hum. Mol. Genet.*, **14**, 1049–1058.

14. Samaco,R.C., Hogart,A. and LaSalle,J.M. (2005) Epigenetic overlap in autism-spectrum neurodevelopmental disorders: MECP2 deficiency causes reduced expression of UBE3A and GABRB3. *Hum. Mol. Genet.*, **14**, 483–492.

15. Jiang,Y.H., Armstrong,D., Albrecht,U., Atkins,C.M., Noebels,J.L., Eichele,G., Sweatt,J.D. and Beaudet,A.L. (1998) Mutation of the Angelman ubiquitin ligase in mice causes increased cytoplasmic p53 and deficits of contextual learning and long-term potentiation. *Neuron*, **21**, 799–811.

16. Miura,K., Kishino,T., Li,E., Webber,H., Dikkes,P., Holmes,G.L. and Wagstaff,J. (2002) Neurobehavioral and electroencephalographic abnormalities in Ube3a maternal-deficient mice. *Neurobiol. Dis.*, **9**, 149–159.

17. Weeber,E.J., Jiang,Y.H., Elgersma,Y., Varga,A.W., Carrasquillo,Y., Brown,S.E., Christian,J.M., Mirnikjoo,B., Silva,A., Beaudet,A.L. and Sweatt,J.D. (2003) Derangements of hippocampal calcium/calmodulin-dependent protein kinase II in a mouse model for Angelman mental retardation syndrome. *J. Neurosci.*, **23**, 2634–2644.

18. Albrecht,U., Sutcliffe,J.S., Cattanach,B.M., Beechey,C.V., Armstrong,D., Eichele,G. and Beaudet,A.L. (1997) Imprinted expression of the murine Angelman syndrome gene, Ube3a, in hippocampal and Purkinje neurons. *Nature Genet.*, **17**, 75–78.

19. Yang,T., Adamson,T.E., Resnick,J.L., Leff,S., Wevrick,R., Francke,U., Jenkins,N.A., Copeland,N.G. and Brannan,C.I. (1998) A mouse model for Prader–Willi syndrome imprinting-centre mutations. *Nature Genet.*, **19**, 25–31.

20. Kashiwagi,A., Meguro,M., Hoshiya,H., Haruta,M., Ishino,F., Shibahara,T. and Oshimura,M. (2003) Predominant maternal expression of the mouse Atp10c in hippocampus and olfactory bulb. *J. Hum. Genet.*, **48**, 194–198.

21. Pfaffl,M.W. (2001) A new mathematical model for relative quantification in real-time RT–PCR. *Nucleic Acids Res.*, **29**, e45.

22. Sivaraman,L., Nawaz,Z., Medina,D., Conneely,O.M. and O'Malley,B.W. (2000) The dual function steroid receptor coactivator/ubiquitin protein-ligase integrator E6-AP is overexpressed in mouse mammary tumorigenesis. *Breast Cancer Res. Treat.*, **62**, 185–195.

23. Kiyosawa,H., Mise,N., Iwase,S., Hayashizaki,Y. and Abe,K. (2005) Disclosing hidden transcripts: mouse natural sense-antisense transcripts tend to be poly(A) negative and nuclear localized. *Genome Res.*, **15**, 463–474.

24. Wevrick,R. and Francke,U. (1997) An imprinted mouse transcript homologous to the human imprinted in Prader–Willi syndrome (IPW) gene. *Hum. Mol. Genet.*, **6**, 325–332.

25. Dhar,M., Webb,L.S., Smith,L., Hauser,L., Johnson,D. and West,D.B. (2000) A novel ATPase on mouse chromosome 7 is a candidate gene for increased body fat. *Physiol. Genomics*, **4**, 93–100.

26. Meguro,M., Kashiwagi,A., Mitsuya,K., Nakao,M., Kondo,I., Saitoh,S. and Oshimura,M. (2001) A novel maternally expressed gene, ATP10C, encodes a putative aminophospholipid translocase associated with Angelman syndrome. *Nature Genet.*, **28**, 19–20.

27. Kayashima,T., Yamasaki,K., Joh,K., Yamada,T., Ohta,T., Yoshiura,K., Matsumoto,N., Nakane,Y., Mukai,T., Niikawa,N. and Kishino,T. (2003)

28. Kayashima,T., Ohta,T., Niikawa,N. and Kishino,T. (2003) On the conflicting reports of imprinting status of mouse ATP10a in the adult brain: strain-background-dependent imprinting? *J. Hum. Genet.*, **48**, 492–493.

29. LaSalle,J.M. and Lalande,M. (1996) Homologous association of oppositely imprinted chromosomal domains. *Science*, **272**, 725–728.

30. Herzing,L.B., Cook,E.H.,Jr and Ledbetter,D. (2002) Allele-specific expression analysis by RNA-FISH demonstrates preferential maternal expression of UBE3A and imprint maintenance within 15q11–q13 duplications. *Hum. Mol. Genet.*, **11**, 1707–1718.

31. Nogami,M., Kohda,A., Taguchi,H., Nakao,M., Ikemura,T. and Okumura,K. (2000) Relative locations of the centromere and imprinted SNRPN gene within chromosome 15 territories during the cell cycle in HL60 cells. *J. Cell. Sci.*, **113**, 2157–2165.

32. Riesselmann,L. and Haaf,T. (1999) Preferential S-phase pairing of the imprinted region on distal mouse chromosome 7. *Cytogenet. Cell Genet.*, **86**, 39–42.

33. Gabriel,J.M., Merchant,M., Ohta,T., Ji,Y., Caldwell,R.G., Ramsey,M.J., Tucker,J.D., Longnecker,R. and Nicholls,R.D. (1999) A transgene insertion creating a heritable chromosome deletion mouse model of Prader–Willi and Angelman syndromes. *Proc. Natl Acad. Sci. USA*, **96**, 9258–9263.

34. Sotomaru,Y., Katsuzawa,Y., Hatada,I., Obata,Y., Sasaki,H. and Kono,T. (2002) Unregulated expression of the imprinted genes H19 and Igf2r in mouse uniparental fetuses. *J. Biol. Chem.*, **277**, 12474–12478.

35. Forne,T., Oswald,J., Dean,W., Saam,J.R., Bailleul,B., Dandolo,L., Tilghman,S.M., Walter,J. and Reik,W. (1997) Loss of the maternal H19 gene induces changes in Igf2 methylation in both *cis* and *trans*. *Proc. Natl Acad. Sci. USA*, **94**, 10243–10248.

36. Hatada,I., Nabetani,A., Arai,Y., Ohishi,S., Suzuki,M., Miyabara,S., Nishimune,Y. and Mukai,T. (1997) Aberrant methylation of an imprinted gene U2af1-rs1(SP2) caused by its own transgene. *J. Biol. Chem.*, **272**, 9120–9122.

37. Duvillie,B., Bucchini,D., Tang,T., Jami,J. and Paldi,A. (1998) Imprinting at the mouse Ins2 locus: evidence for *cis*- and *trans*-allelic interactions. *Genomics*, **47**, 52–57.

38. Rassoulzadegan,M., Magliano,M. and Cuzin,F. (2002) Transvection effects involving DNA methylation during meiosis in the mouse. *EMBO J.*, **21**, 440–450.

39. Herman,H., Lu,M., Anggraini,M., Sikora,A., Chang,Y., Yoon,B.J. and Soloway,P.D. (2003) *Trans* allele methylation and paramutation-like effects in mice. *Nature Genet.*, **34**, 199–202.

40. Tsai,T.F., Bressler,J., Jiang,Y.H. and Beaudet,A.L. (2003) Disruption of the genomic imprint in *trans* with homologous recombination at Snrpn in ES cells. *Genesis*, **37**, 151–161.

41. Wood,A., Krogan,N.J., Dover,J., Schneider,J., Heidt,J., Boateng,M.A., Dean,K., Golshani,A., Zhang,Y., Greenblatt,J.F. *et al.* (2003) Bre1, an e3 ubiquitin ligase required for recruitment and substrate selection of rad6 at a promoter. *Mol. Cell*, **11**, 267–274.

42. Rosok,O. and Sioud,M. (2004) Systematic identification of sense–antisense transcripts in mammalian cells. *Nat. Biotechnol.*, **22**, 104–108.

43. Shibata,S. and Lee,J.T. (2003) Characterization and quantitation of differential Tsix transcripts: implications for Tsix function. *Hum. Mol. Genet.*, **12**, 125–136.

44. Shibata,S. and Lee,J.T. (2004) Tsix transcription- versus RNA-based mechanisms in Xist repression and epigenetic choice. *Curr. Biol.*, **14**, 1747–1754.

Atp10a, the mouse ortholog of the human imprinted ATP10A gene, escapes genomic imprinting. *Genomics*, **81**, 644–647.